

Optical phonons in isotopic Ge studied by Raman scattering

J. M. Zhang, M. Gehler,* A. Göbel, T. Ruf, and M. Cardona

Max-Planck-Institut für Festkörperforschung, Heisenbergstraße 1, D-70569 Stuttgart, Germany

E. E. Haller and K. Itoh

Lawrence Berkeley National Laboratory and University of California, Berkeley, California 94720

(Received 28 August 1997)

The effects of isotopic substitution on the Γ -point phonon in isotopically enriched (^{70}Ge , ^{73}Ge , ^{74}Ge , and ^{76}Ge) and disordered (natural Ge and $^{70/76}\text{Ge}$) germanium samples have been measured with Raman spectroscopy. We believe, in contrast to earlier work, that intrinsic bulk Raman phonons are observed only when surface oxides are removed by chemical etching, and a laser line in the red is used to greatly enhance the penetration depth of the light. In high-resolution experiments at 10 K, performed under these conditions, we obtain more precise phonon frequencies and find significantly reduced phonon linewidths than reported before. Our observations improve on previous results, and are in better agreement with predictions of coherent-potential-approximation and supercell calculations. [S0163-1829(98)00204-5]

I. MOTIVATION

Germanium has a wide range of stable isotopes spanning from ^{70}Ge to ^{76}Ge . Intensive studies of the isotope effects in Ge have been performed in the past few years, since large enough affordable quantities of highly enriched stable isotopes became available.¹⁻³ Using high-resolution Raman spectroscopy, Fuchs *et al.* measured the average-mass dependence of phonon frequencies and linewidths at the Γ point for some isotopically enriched Ge samples, natural Ge, and a highly disordered $^{70/76}\text{Ge}$ alloy.^{4,5} The isotopically enriched samples show a frequency inversely proportional to the square root of the average mass, and a linewidth inversely proportional to the mass, in agreement with the harmonic approximation and Fermi's golden rule, respectively. However, in natural Ge and the $^{70/76}\text{Ge}$ alloy isotope, disorder causes an additional shift of the phonon frequency and a broadening of the linewidth. These effects can be explained within the framework of self-energy calculations based on the coherent-potential approximation (CPA).

Because of the small band gap in Ge (the indirect gap at 6 K is $E_g=0.74$ eV),⁶ and the low frequency of the strongly absorbing E_1 critical point (2.25 eV at 6 K),⁶ light in the visible is attenuated rapidly. The absorption coefficient α , at 5145 Å, where most experiments have been performed so far, is as high as $6 \times 10^5 \text{ cm}^{-1}$ at 100 K.⁷ This leads to an effective penetration depth $1/2\alpha$ of only 8 nm, comparable to the typical thickness of oxide films on Ge surfaces prepared only by polishing (~ 1 nm).^{7,8} Raman measurements at this wavelength are therefore very sensitive to surface effects. Surface stress and enhanced nonradiative recombination at the Ge-oxide interface cause an inhomogeneous line broadening and a reduction of the signal intensity. They should thus be avoided for precise measurements of isotope effects.

In this work, we present the Raman spectra of isotopically pure (^{70}Ge , ^{73}Ge , ^{74}Ge , and ^{76}Ge) and disordered (natural Ge and $^{70/76}\text{Ge}$) samples, measured with the 6471 and 6764 Å Kr-ion laser lines. At these wavelengths the samples have much larger penetration depths than at 5145 Å (64 and 87

nm, respectively, calculated with the optical parameters measured at 100 K).⁷ In addition, the samples were chemically etched immediately before the Raman measurements to minimize the surface oxide thickness. This allows us to observe basically bulk phonons, and constitutes the starting point for a reinvestigation of the isotope effects in Ge. The measured data improve on the previous experimental results, and compare well with recent theoretical calculations.^{12,16}

II. EXPERIMENT

The isotopically pure samples, except for a ^{73}Ge crystal, are the same as those used before.^{4,5,9} The surfaces investigated have the (111) orientation. The alloy sample, $^{70/76}\text{Ge}$, has been grown in order to maximize the isotope disorder. This sample was cut to obtain a (100)-oriented surface. Its isotopic composition was determined with mass spectroscopy as ^{70}Ge (42.7%), ^{72}Ge (2.1%), ^{73}Ge (<0.1%), ^{74}Ge (7.2%), and ^{76}Ge (48.0%) (accuracy $\pm 0.5\%$). Three natural Ge samples were cut from the same crystal in the (100), (110), and (111) orientations, respectively. High-quality surfaces for Raman measurements were prepared by chemomechanical polishing with SYTON which was performed in an identical way for all of the Ge samples. The surfaces were further etched for about 2 min in 5% HF aqueous solution to remove the oxide films immediately prior to the measurements.^{7,8,10,11}

Raman measurements were performed in the usual back-scattering configurations using the 5145, 6471, or 6764 Å laser lines from either an Ar- or a Kr-ion laser with excitation powers of 100 mW and a line focus. We verified that sample heating can be neglected. High resolution was achieved by measuring in the 11th (for 5145 Å excitation) or eighth (for the 6471 and 6764 Å excitations, respectively) diffraction order of the 316 groves/mm echelle gratings of a $f=2.0$ m SOPRA (Société de Production et de Recherches Appliquées) double monochromator (model DMDP 2000). An $f=0.85$ m double monochromator (model SPEX 1404) with 1800 groves/mm holographic gratings was also used for

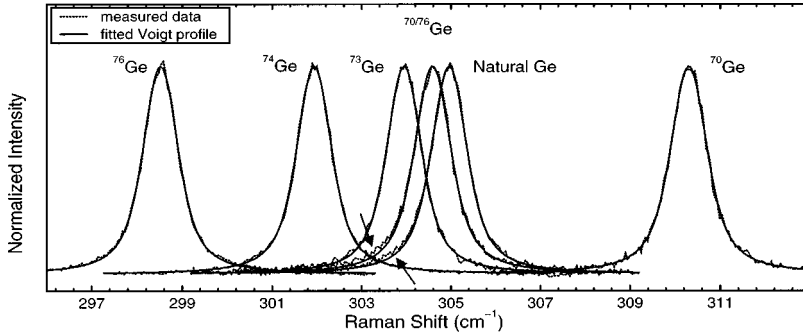


FIG. 1. High-resolution Raman spectra of isotopically enriched and disordered Ge (as marked in the figure). The spectra were taken at 10 K with 6471 Å excitation. Arrows point to the low-energy shoulders in the spectra of natural Ge and $^{70/76}\text{Ge}$ alloy samples.

the measurements. With very narrow slit widths and long integration times the required high resolution can also be achieved on this instrument. The scattered light was detected by single-photon counting. A nearby emission line from a neon lamp was always measured together with the Raman peaks from the Ge samples in order to obtain a precise calibration of the frequency scale. The phonon lines were measured several times for each sample.

III. RESULTS AND DISCUSSION

Figure 1 shows the Raman spectra of the isotopically pure and disordered Ge samples at 10 K, measured with an excitation of 6471 Å. The spectra are normalized in intensity, and constant backgrounds were subtracted for the sake of comparison. The dotted lines represent experimental data, while the solid lines are fits with Voigt profiles which correspond to the convolution of a Lorentzian phonon peak with the Gaussian instrumental profile.¹¹ A fixed width of 0.43 cm^{-1} full width at half maximum, used for the Gaussian component in these fits, was obtained by measuring the spectrum of the laser line under identical conditions as the phonon peaks. In contrast to the case of the 2.41 eV excitation,⁴ spectra of the isotopically pure samples (^{70}Ge , ^{73}Ge , ^{74}Ge , and ^{76}Ge) can be well fitted by Voigt line shapes without obvious low-energy tails. The tails persist, however, in the two disordered samples, as indicated by the arrows in Fig. 1.

Two processes are responsible for asymmetric Raman line shapes in Ge:^{4,12} (i) isotopic disorder contributions to the frequency-dependent self-energy; and (ii) absorption of laser light which occurs even in isotopically pure samples. In addition to an asymmetric broadening of the Raman line, isotope disorder also leads to pronounced tails reflecting the phonon density of states 10–20 cm^{-1} below the Γ -point phonon frequency.⁵ Strong absorption of the laser light leads to a corresponding spread in the wave vector \mathbf{q} . As a result ($\mathbf{q} \neq 0$) phonons on the lower-frequency side of the Γ -point phonon can be observed. When the samples are excited with the 5145 Å laser line, the second process makes the dominant contribution to the low-energy tail because of the very strong absorption. This can be seen in the spectra of natural Ge samples with different orientations shown in Fig. 2(a). For the polarization chosen, only LO (Γ -X), TO (Γ -L), and TO (Γ -K) phonons are observed in the (100)-, (111)-, and (110)-oriented samples, respectively.¹³ The curvature of the phonon dispersion around the Γ point increases when going from LO (Γ -X) to TO (Γ -L), and further to TO (Γ -K).¹⁴ This explains the significant enhancement of the asymmetry in the spectra of Fig. 2(a) from the bottom to the top. The

asymmetry almost vanishes when the spectra are measured with the red laser lines. As shown in Fig. 2(b), much weaker low-energy shoulders with similar intensities for all three directions are then found in this series of natural Ge samples. The reduction of the absorption coefficient by almost one order of magnitude when the samples are excited with the red laser lines (6471 Å: $\alpha = 7.8 \times 10^4 \text{ cm}^{-1}$; 6764 Å: $\alpha = 5.8 \times 10^4 \text{ cm}^{-1}$) results in a much slower spatial decay of the incident laser light. From the phenomenological one-dimensional model,⁴ the half-width of the wave-vector spread due to the attenuation of light, which is equal to the absorption coefficient α , thus decreases from 0.54% at 5145 Å, to 0.07% and 0.05% of the length of Brillouin zone ($2\pi/a$) at 6471 and 6764 Å, respectively. As a result, much fewer ($\mathbf{q} \neq 0$) phonons contribute to the Raman spectrum. The absorption-induced line-shape asymmetry vanishes, while almost only the isotopic-disorder-induced low-energy shoulder persists. In addition, we have found small but systematic differences of the phonon linewidths in natural Ge samples with different orientations. Measurements with the 6471 Å laser line as in Fig. 2(b) yield $\Gamma = 0.66(2)$, $0.63(2)$, and $0.64(2) \text{ cm}^{-1}$ for (100)-, (110)-, and (111)-oriented natural Ge. These differences in linewidth, although marginal, seem to be real. They are not yet fully understood. Significant differences in phonon line shapes for the various scattering surfaces were reported in Ref. 15. However, they only occur above the E_1 gap ($\approx 2.2 \text{ eV}$), i.e., in the presence of strong absorption. It is therefore unlikely that the proposed origin of these differences (a double resonance at the E_1 gap) (Ref.

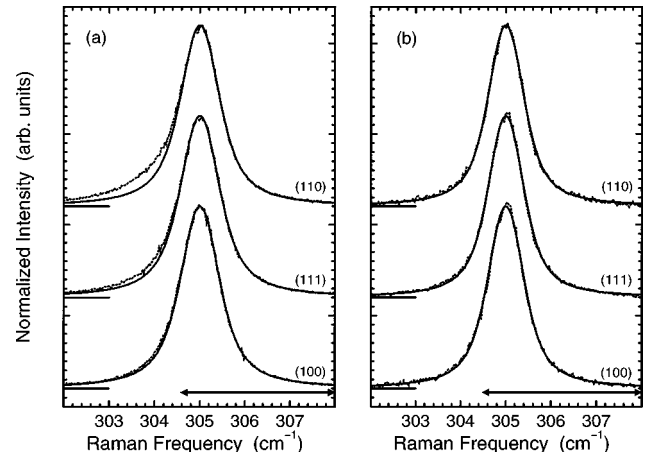


FIG. 2. Raman spectra of natural Ge (dashed lines) with different orientations as indicated. The spectra were taken at 10 K with 5145 Å (a) and 6471 Å (b) excitations. The fits (solid lines) were performed only in the regions defined by the arrows.

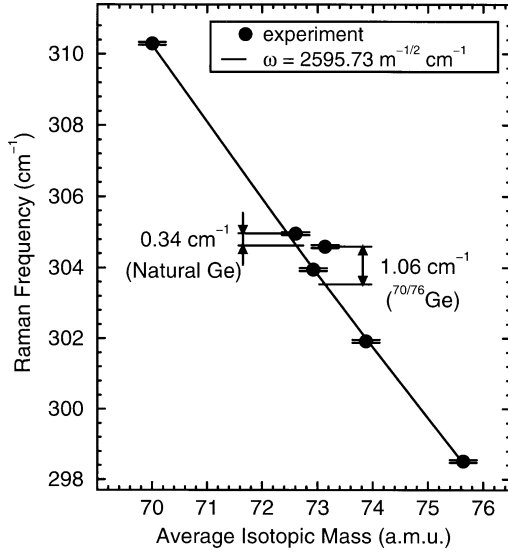


FIG. 3. Raman frequency as a function of the average mass, measured at 10 K, for isotopically enriched and disordered Ge samples. The solid line is a calculation with $\omega = 2595.73/\sqrt{m}$ cm^{-1} .

15) can explain the observations reported here. More work is needed to elucidate the differences in linewidth reported here, and their possible dependence on laser frequency.

Figure 3 shows the measured Raman frequency shifts of the Ge samples versus the average mass. For the isotopically pure Ge samples, the phonon frequencies follow an $\omega \sim 1/\sqrt{m}$ behavior, indicated by the solid line, within the experimental errors. This behavior is expected within the harmonic approximation.^{1,4} Additional frequency shifts are observed for the natural and alloy samples which arise from their isotope mass disorder. This additional shift is $0.34 \pm 0.04 \text{ cm}^{-1}$ in natural Ge, and $1.06 \pm 0.04 \text{ cm}^{-1}$ in the $^{70/76}\text{Ge}$ alloy sample, which has nearly the maximum isotopic disorder possible with natural isotopes. Recent single-site CPA calculations, based on the density of states obtained within the harmonic approximation, predict that the disorder-induced frequency shift of the Γ -point optical phonon amounts to $(0.4 \pm 0.1) \text{ cm}^{-1}$ for natural Ge, and $(1.2 \pm 0.1) \text{ cm}^{-1}$ for the alloy sample, depending on the lattice-dynamical model used to obtain the phonon density of states.¹⁶ A 216-atom supercell lattice-dynamical simulation predicts these values to be (0.3 ± 0.2) and $(1.1 \pm 0.2) \text{ cm}^{-1}$, respectively.¹⁶ A simple estimate from second-order perturbation theory can also provide a reasonable prediction of these disorder-induced frequency shifts.^{12,17} The disorder-induced frequency shift is given by

$$\Delta\omega = g_2 \frac{\omega^3}{12} \int_0^\infty \frac{1}{\omega^2 - \omega_i^2} N_d(\omega_i) d\omega_i, \quad (1)$$

where the phonon density of states (the measured data¹⁸ are chosen here) are normalized through $\int_0^\infty N_d(\omega_i) d\omega_i = 6$. The mass-fluctuation parameter g_2 is given by

$$g_2 = \sum_i x_i \left(1 - \frac{m_i}{\bar{m}} \right)^2, \quad (2)$$

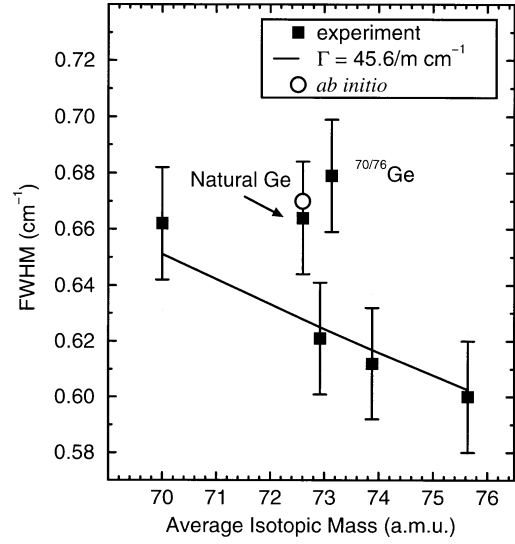


FIG. 4. Intrinsic phonon linewidth of isotopic Ge vs the average mass, measured at 10 K, with an excitation of 6471 \AA . The *ab initio* linewidth reported in Ref. 20 for isotopically pure Ge with $m = 72.6$ is indicated by the circle.

where x_i is the fraction of isotope i , m_i its mass, and \bar{m} the average mass. This equation yields $g_2 = 5.87 \times 10^{-4}$ for natural Ge and $g_2 = 1.53 \times 10^{-3}$ for the alloy, respectively. Using Eq. (1) we obtain a disorder-induced frequency shift of 0.41 cm^{-1} for the natural sample, and 1.07 cm^{-1} for the $^{70/76}\text{Ge}$ alloy sample, respectively.

The experimental values of our reinvestigated phonon frequencies and linewidths are more precise than the previous ones, and in better agreement with the calculations. The disorder-induced frequency shift had been reported to be 0.74 cm^{-1} for natural Ge and 0.98 cm^{-1} for the $^{70/76}\text{Ge}$ alloy.^{4,9,19} The value in the natural sample evidently deviates from the predictions, since the additional frequency shift should be proportional to the mass-fluctuation parameter g_2 . Thus the disorder-induced frequency shift is expected to be larger by a factor of about 2.6 in the alloy than in natural Ge. This is observed in the experiments reported here, and also predicted by the full CPA and supercell calculations.¹⁶

The phonon linewidths measured with red laser lines are significantly smaller than the ones obtained with 5145 \AA , both in the present work and in previous reports.⁴ In (111)-oriented natural Ge we find a full width at half maximum (FWHM) of $0.87 \pm 0.02 \text{ cm}^{-1}$ when chemical polishing with SYTON is performed prior to the measurement and the 5145 \AA laser line is chosen. This value decreases to $0.76 \pm 0.02 \text{ cm}^{-1}$ after chemical etching with HF, and further to $0.66 \pm 0.02 \text{ cm}^{-1}$ when the 6471 \AA laser line is used. The last number is in excellent agreement with the *ab initio* prediction reported in Ref. 20, which gives a linewidth of 0.67 cm^{-1} for isotopically pure Ge with $m = 72.6$. This result confirms our hypothesis: because of the strong absorption in the visible, the measured phonon line shapes are strongly affected by surface oxide films, which have a thickness comparable to the penetration depth of the light, and by contributions from phonons with nonzero \mathbf{q} vector near the Brillouin zone center. The present data are therefore much closer to the intrinsic phonon linewidth in bulk Ge, since the oxide films were removed and the penetration depth is much larger.

Figure 4 shows the FWHM versus the average atomic mass in isotopic Ge, measured with etched surfaces and an excitation of 6471 Å. Within the experimental error, determined from several measurements, the linewidths of the isotopically pure Ge samples decrease with increasing average mass. This behavior, shown by the solid line in the figure, is well described by $\Gamma = 45.6/\bar{m}$, and can be explained by Fermi's golden rule.^{1,4} The broadening of the phonon lines due to the anharmonic decay through three-phonon interaction is proportional to the interaction strength ($\sim \bar{m}^{-3/2}$) and the two-phonon joint density of states ($\sim \bar{m}^{1/2}$).²¹ This yields the $\Gamma \sim 1/\bar{m}$ law at zero temperature, in good agreement with the experimental data for the isotopically pure samples.

An additional broadening [(0.03±0.03) cm⁻¹ for natural Ge, and (0.06±0.03) cm⁻¹ for the alloy sample] is clearly seen in the two isotopically mixed samples. Their linewidths lie significantly above those expected from the inverse-average-mass rule. This can be attributed to a combination of disorder-induced scattering and anharmonic decay. Including the anharmonic broadening in the phonon density of states, $N_d(\omega)$, yields a nonvanishing scattering probability on the mass defects. One can thus estimate the mass-disorder-induced broadening of the optical phonon with the expression³

$$\Gamma_{\text{isotope}} = g_2 \frac{\pi \omega^2}{12} N_d(\omega). \quad (3)$$

This calculation gives an additional broadening of 0.017 cm⁻¹ for natural Ge, and of 0.046 cm⁻¹ for the ⁷⁰Ge_{0.5}⁷⁶Ge_{0.5} alloy, in agreement with the measured data.

IV. CONCLUSION

In summary, nominally intrinsic Ge phonons can be observed in Raman spectroscopy using an excitation line in the red to enhance the penetration depth of the light, and a chemical etching of the sample surface. This leads to a significant decrease of the measured linewidths, and to more precise data for the phonon frequency shifts with isotope substitution. Using this advantage we have reinvestigated the isotope effects on the Γ -point phonon in isotopically pure (⁷⁰Ge, ⁷³Ge, ⁷⁴Ge, and ⁷⁶Ge) and disordered (natural Ge and ^{70/76}Ge) samples. The observations improve on the previous results and are now in better agreement with CPA and supercell calculations.

ACKNOWLEDGMENTS

We thank C. Ulrich for his help on the chemical etching and discussions. Thanks are due to M. Siemers, H. Hirt, and P. Hiebl for technical assistance. This work was supported in part by an INTAS grant. One of the authors (J. M. Z.) gratefully acknowledges financial support from the Max-Planck-Gesellschaft. Thanks are also due to A. Cantarero for a careful reading of the manuscript.

*Permanent address: Paul-Drude-Institut für Festkörperelektronik, Hausvogteiplatz 5-7, D-10117 Berlin, Germany.

¹M. Cardona, in *Festkörperprobleme/Advances in Solid State Physics*, edited by R. Helbig (Vieweg, Braunschweig, 1994), Vol. 34, p. 35; see also T. Ruf, H. Fuchs, and M. Cardona, *Phys. Bl.* **52**, 1115 (1996).

²E. E. Haller, *J. Appl. Phys.* **77**, 2857 (1995).

³M. Cardona, *J. Phys. Condens. Matter* **5**, A61 (1993).

⁴H. D. Fuchs *et al.*, *Phys. Rev. B* **44**, 8633 (1991).

⁵H. D. Fuchs *et al.*, *Phys. Rev. Lett.* **70**, 1715 (1993).

⁶C. Parks *et al.*, *Phys. Rev. B* **49**, 14 244 (1994).

⁷L. Viña, S. Logothetidis, and M. Cardona, *Phys. Rev. B* **30**, 1979 (1984).

⁸R. J. Archer, *Phys. Rev.* **110**, 354 (1958); *J. Electrochem. Soc.* **104**, 619 (1957).

⁹P. Etchegoin *et al.*, *Phys. Rev. B* **48**, 12 661 (1993).

¹⁰D. E. Aspnes and A. A. Studna, *Appl. Phys. Lett.* **39**, 316 (1981).

¹¹C. Ulrich *et al.*, *Phys. Rev. Lett.* **78**, 1283 (1997).

¹²D. T. Wang *et al.*, in *The Physics of Semiconductors*, edited by

M. Scheffler and R. Zimmermann (World Scientific, Singapore, 1996), p. 197; D. T. Wang *et al.*, *Phys. Rev. B* **56**, 13 167 (1997).

¹³M. Cardona, in *Light Scattering in Solids II*, edited by M. Cardona and G. Güntherodt, *Topics in Applied Physics* Vol. 50 (Springer, Berlin, 1982), p. 19.

¹⁴G. Nilsson and G. Nelin, *Phys. Rev. B* **3**, 364 (1971).

¹⁵D. J. Mowbray *et al.*, in *Proceedings of the 20th International Conference on the Physics of Semiconductors*, edited by E. M. Anastassakis and J. D. Joannopoulos (World Scientific, Singapore, 1990), p. 2017.

¹⁶A. Göbel *et al.* (unpublished).

¹⁷J. Menéndez, J. B. Page, and S. Guha, *Philos. Mag. B* **70**, 651 (1994).

¹⁸G. Nelin and G. Nilsson, *Phys. Rev. B* **5**, 3151 (1972).

¹⁹H. D. Fuchs *et al.*, *Solid State Commun.* **82**, 225 (1992).

²⁰A. Debernardi, S. Baroni, and E. Molinari, *Phys. Rev. Lett.* **75**, 1819 (1995).

²¹J. Menéndez and M. Cardona, *Phys. Rev. B* **29**, 2051 (1984).